

Contents lists available at ScienceDirect

Carbohydrate Polymer Technologies and Applications

journal homepage: www.sciencedirect.com/journal/carbohydrate-polymer-technologies-and-applications



Pyridine catalyzed acylation of electrospun chitosan membranes by C6-C12 acyl chlorides: Effect of reaction time and chain length

Rabeta Yeasmin^a, Ezzuddin Abuhussein^a, Felio Perez^b, Tomoko Fujiwara^c, Joel D Bumgardner^a, Jessica Amber Jennings^{a,*}

- ^a Department of Biomedical Engineering, The University of Memphis, Memphis, TN 38152, USA
- ^b Department of Biology, The University of Memphis, Memphis, TN 38152, USA
- ^c Department of Chemistry, The University of Memphis, Memphis, TN 38152, USA

ARTICLEINFO

Keywords: Chitosan Electrospun membrane O-acylation Reaction time Acyl chloride

ABSTRACT

Chitosan nanofiber membranes manufactured via electrospinning are attractive for drug delivery applications due to their increased surface area. The as-spun fibers contain trifluoroacetate (TFA)-salts that cause swelling and loss of nanofiber structure in physiological solutions and are cytotoxic. Here, a post-electrospinning treatment has been reported using fatty acyl chlorides and pyridine to O-acylate the membranes with different acyl chainlength (C6, C8, C10, and C12). The O-acylation reactions were carried out with acyl chlorides in a basic environment for 2 hr, 3 hr, 4 hr and, 5 hr. The effects of the acyl chain length and the reaction time were assessed using various physio-chemical characterization techniques including FTIR, NMR, Contact Angle, XPS, and SEM. The acylated nanofibers displayed hydrophobic properties and allowed the removal of the cytotoxic TFA salts without compromising the nanofibrous structure. The fiber diameter increased with the increasing length of the substituted acyl chain. The degree of substitution of the acyl chains did not change significantly when reacted for a longer period indicating the completion of the reaction within 2 hr. This could allow the faster modification of the membranes for potential application in the delivery of hydrophobic drugs.

Introduction

Chitosan is a biopolymer obtained through an N-deacetylation of chitin, a natural polysaccharide similar in structure to cellulose. Deacetylation removes the acetamide group exposing the amine group which makes chitosan soluble in dilute acids and more chemically active than chitin. The structure of chitosan consists of N-acetyl glucosamine units and deacetylated glucosamine units linked through β -(1,4)-glycosidic bonds (Novikov, Derkach, Konovalova, Dolgopyatova & Kuchina, 2023). The relative ratio of glucosamine units to N-acetyl glucosamine units is referred to as degree of deacetylation (DDA), and it can significantly affect chitosan's activities. Chitosan is widely used in biomedical applications due to its properties such as cytocompatibility, biodegradability, antimicrobial effects, and wound healing (Borsagli, Carvalho & Mansur, 2018). Electrospinning has been recognized as an efficient way of fabricating nanofibers by applying a high-voltage electric field to a charged polymeric solution. The advantage of having fibers within the micrometer to nanometer range is the increased surface area

which is suitable for drug delivery. Furthermore, the nanofibrous matrix resembles the extracellular matrix (ECM) in structure and simulates the differentiation capabilities of different kinds of human cells including osteoblasts, chondrocytes, and cartilage (Lahiji, Sohrabi, Hungerford & Frondoza, 2000; Lin et al., 2020).

Chitosan can be electrospun in multiple solvent systems such as concentrated acetic acid solutions, hydrochloric acids, and formic acid where the resulting electrospun chitosan membranes have homogenous structures without beads (Ravi Kumar, 2000). However, the diameter and morphology of fibers varies with the type and ratio of solvents used. For example, a strong acetic acid solution (90 %) with a 3 % chitosan concentration resulted in membranes that are 70 nm in diameter whereas an acetic acid concentration of 30 % produces a fiber diameter of 40 nm (Geng, Kwon & Jang, 2005; Piechota, Kot, Frankowska-Maciejewska, Gruz ewska & Wo zniak-Kosek, 2018). Ohkawa et al. achieved successful electrospinning of chitosan using trifluoroacetic acid (TFA) since TFA has a high volatility and therefore solidifies the jet of the chitosan-TFA solution. The authors added

https://doi.org/10.1016/j.carpta.2024.100443

^{*} Corresponding author.

E-mail address: jjnnings@memphis.edu (J.A. Jennings).

dichloromethane (DCM) to increase volatility and found that 70:30 ratio of TFA: DCM is the ideal ratio to achieve bead-free nanofibers (Ohkawa, Cha, Kim, Nishida & Yamamoto, 2004). Despite the success of their method, TFA salts formed with the amine group are very cytotoxic and not suitable for biomedical applications. The removal of these salts has been a challenge since the nanofibrous structure is easily compromised using the typical extraction methods and causes swelling due to the hydrophilic nature of the functional groups (Homayoni, Ravandi & Valizadeh, 2009). Chemically modified electrospun chitosan improves its physical and chemical properties for its applications (Borsagli et al., 2018). Furthermore, since the nanofibrous structure is not stable in aqueous mediums because of the ionic TFA salt, modifying chitosan membrane to achieve hydrophobicity allows the safe removal of the TFA salts.

Acylation is a common technique to incorporate fatty acid chains with the electrospun membrane to increase its hydrophobicity. The main active functional groups in chitosan are C₃-OH, C₆-OH, and C₂-NH₂, creating two possibilities for acylation: N-acylation and Oacylation. The primary hydroxyl group at C₆ has low steric hindrance, making its reactivity higher than the secondary hydroxyl group at C₃ which is not able to rotate in the spatial conformation. The C2-NH2 group has the highest activity allowing for the formation of an amide. However, the amine group in the electrospun membrane is less accessible for acylation due to the existing ammonium TFA salt. Wu et al. introduced an O-acylation method using acyl anhydride and pyridine to successfully attach fatty acid chains and subsequently remove TFA salt by washing with water (Chaoxi Wu, Su, Tang & Bumgardner, 2014). Zhang et al. synthesized O-acylated chitosan nanofibers with 2 - 12 carbon chain lengths using the same technique and found that the hydrophobicity increases with the increased length of the substituted acyl groups (Zhen Zhang et al., 2017). Furthermore, the chitosan nanofibers acylated using fatty acyl anhydrides can control the release of hydrophobic drug simvastatin and supports osteogenic differentiation facilitating bone healing in guided bone regeneration applications (Murali et al., 2020, 2021). However, some novel fatty acids are not commercially available as anhydrides such as trans-2-decenoic acid, cis-2-decenoic acid, and 2-heptylcyclopropane-1-carboxylic acid which are biologically very promising for their antibiofilm activity and can be incorporated with nanofibers as a potential therapy for infection. Wells et al. studied another O-acylation technique using acyl chloride and pyridine along with a custom synthesis route of acyl chloride to graft commercially unavailable fatty acids (Wells et al., 2021). Chitosan flakes have been directly acylated using acyl chlorides as well, but the overall process was complex and slow since chitosan is not very reactive due to its extensive intramolecular hydrogen bonding (Fujii, Kumagai & Noda, 1980; Grant, Blair & Mckay, 1990; Le Tien, Lacroix, Ispas-Szabo & Mateescu, 2003; Zong, Kimura, Takahashi & Yamane, 2000). Further, it is difficult to generate fine and uniform nanofibers via electrospinning these chitosan derivatives due to the steric hindrance rendered by the long side chains. For example, electrospun membranes fabricated directly from hexanoyl chitosan exhibited a wide range of fiber diameters of $0.64-3.93 \mu m$.

This present study investigates post-electrospinning modifications using different chain-length (C6, C8, C10, and C12) acyl chlorides and different reaction times to achieve O-acylation. Material characteristics of the different modification types such as fiber morphology, degree of substitution, and hydrophobicity were characterized and compared.

Experimental section

Materials

Chitosan (86.5 % DDA, MW=664.7 kDa, intrinsic viscosity=6.249 dL/g) was purchased from ChitoLytic Inc. (ON, Canada). Trifluoracetic acid (TFA), dichloromethane (DCM), hexanoyl chloride, octanoyl chloride, decanoyl chloride, and dodecanoyl chloride were purchased from

Sigma Aldrich (MO, USA). Pyridine and acetone were purchased from Fisher Scientific Inc. (NH, USA).

Preparation of membranes

The nanofibrous membranes were made using the electrospinning technique described in previous publications (Norowski et al., 2012; Norowski, Jr. et al., 2015; Wells et al., 2021; Chaoxi Wu et al., 2014). Briefly, chitosan was dissolved in a mixed solvent of TFA and DCM (7:3 v/v) overnight to make 5.5 wt% solution. The solution was electrospun at a rate of 0.03 ml/min under 25 kV voltage, and the fibers were collected on a 15 cm diameter plate covered with aluminum foil until an approximate thickness of 0.7 mm was reached.

Acylation

The membranes were punched into 10 mm diameter discs, weighed, and placed in each beaker designated for different chlorides. Pyridine was added to the membranes at 10 g membrane/L ratio. Hexanoyl chloride, octanoyl chloride, decanoyl chloride, and dodecanoyl chloride were then added slowly to the respective beakers at a ratio of 1:4 (v/v) to pyridine while continuously stirring. After 2 hrs, 3 hrs, 4 hrs and 5 hrs, one-fourth of the total membrane discs were removed from the beaker and washed with acetone (2.5 g membrane/L) for 10 min followed by three washes with deionized water at 24 h intervals. The membranes were lyophilized in a freeze dryer (Labconco, MO, USA).

Fourier transform infrared spectroscopy (FTIR)

FTIR spectra of the chitosan powder, as-spun membrane, and the acylated membranes were recorded on an Attenuated Total Reflection (ATR) system (PerkinElmer Frontier Universal ATR, MA, USA) with a diamond crystal in the range of $500~\rm cm^{-1}$ to $4000~\rm cm^{-1}$ and at a resolution of $4~\rm cm^{-1}$.

X-ray electron spectroscopy (XPS)

Analysis of the samples were performed using a Thermo Scientific K-Alpha XPS system equipped with a monochromatic X-ray source at 1486.6 eV, corresponding to the Al Ka line. The X-ray power of 75 W at 12 kV was used for all experiments with a spot size of 400 μ m². The base pressure of the K-Alpha instrument was 7.5×10^{-10} mbar. The instrument was calibrated to give a binding energy of 84.0 eV for Au 4f_{7/2} and 284.6 eV for the C1s line of adventitious (aliphatic) carbon present on the non-sputtered samples. Photoelectrons were collected from a takeoff angle of 90° relative to the sample surface.

XPS spectra were collected in the Constant Analyzer Energy mode. The survey spectra were collected at a pass energy of 200 eV and an energy step size of 1.0 eV, while the high resolution (HR) core level spectra of C 1 s, N 1 s were taken at a 40 eV passes energy, an energy step size of 0.1 eV, and using an average of 40 scans. The XPS data acquisition was performed using the Avantage (v5.995) software provided with the instrument. Measurements were taken at three spots per sample from each treatment group.

The degree of substitution of the acylated chain was estimated from the XPS elemental analysis using the following equation:

$$C: N = (6 + px) \times 0.865 + (8 + px) \times 0.135$$
 (1)

Where C and N are the atomic percentages of carbon and nitrogen respectively, x is the degree of substitution, and p is the number of carbon atoms in the acyl chain. The equation was modified from Zhang et al. to consider the respective degree of deacetylation (86.5 %) of the chitosan. (Zhang et al., 2017)

Proton nuclear magnetic resonance (1H NMR)

Around 20 mg of hexanoyl, octanoyl, decanoyl and dodecanoyl modified membranes (5hr reaction group) were dissolved separately in 1 ml of trifluoroacetic acid-d/chloroform-d (TFA-d/CDCl3) (2:1) solvent overnight and ¹H NMR spectra were recorded using JOEL 400 MHz NMR spectrophotometer at room temperature.

Scanning electron microscopy (SEM)

The surface morphology and structure of the nanofiber were examined by scanning electron microscope (Nova NANOSEM 650 FEITM, OR USA) at different resolutions, 5000x images are shown here and lower resolution images at 2500x are attached in the supplementary information. The samples were coated with 5 nm layer of Au and Pd (8:2 w/w) by an ion sputter coater (EMS Quorum/Q 150T ES plus) prior to the scanning.

Three samples from each group were examined and two points from each sample were imaged for fiber diameter measurement. Twenty-five fibers were randomly selected from each 5000x image, therefore a total of 150 fiber diameters from each group were measured manually using ImageJ software (v1.53k).

Water contact angle measurement

Water contact angle of the acylated membranes from 2 h, 3 h, 4 h and, 5 h reaction time points were determined using VCA Optima equipment (AST products, INC, USA). A water droplet of 5μ l was placed carefully on the membrane surface, and a digital camera recorded the image of the droplets approximately after one minute. The contact angle was calculated using the goniometry software of the VCA Optima XE and

six different membranes from each acyl chain and time groups were tested.

Statistical analysis

Statistical analyses were performed on carbon content (n = 3), DS (n = 3), contact angle (n = 6), and fiber diameter (n = 150) using GraphPad Prism 9.4.1 software. The data were tested for normality using the Shapiro-Wilk test, followed by Brown-Forsythe equal variance test. If both passed, the groups were further analyzed with a two-way analysis of variance (ANOVA) followed by Tukey's post-hoc analysis to detect significant differences between experimental groups ($\alpha = 0.05$). If normality and equal variance were not passed, data were analyzed using Kruskal-Wallis ANOVA on ranks, followed by a Tukey's post-hoc test.

Results and discussion

The goal of this study is to determine the time of the acylation reaction to get the maximum degree of substitution of acyl chains in the electrospun chitosan membrane, as well as to check the effect of the chain length and the time of the reaction on the physiochemical characteristics of the membrane. To confirm the acylation and removal of TFA salts, FTIR and XPS were performed on the membrane.

The FTIR spectra in Fig. 1 show that both as-spun chitosan membrane and acylated membranes have peaks at 1650 cm⁻¹ (for amide C = O stretching) and a broad band around 3400 cm⁻¹ corresponding hydrogen bonded N-H and -OH vibrational stretching similar to chitosan powder (Berlanga, Gomez-Perez & Guerrero, 2017). In addition to that, the as-spun membrane has peaks around 722, 802, 841, 1140, 1200 cm⁻¹ and a large peak at 1670 cm⁻¹, which correspond to the trifluoroacetate anions (Chaoxi Wu et al., 2014). The differences in peaks

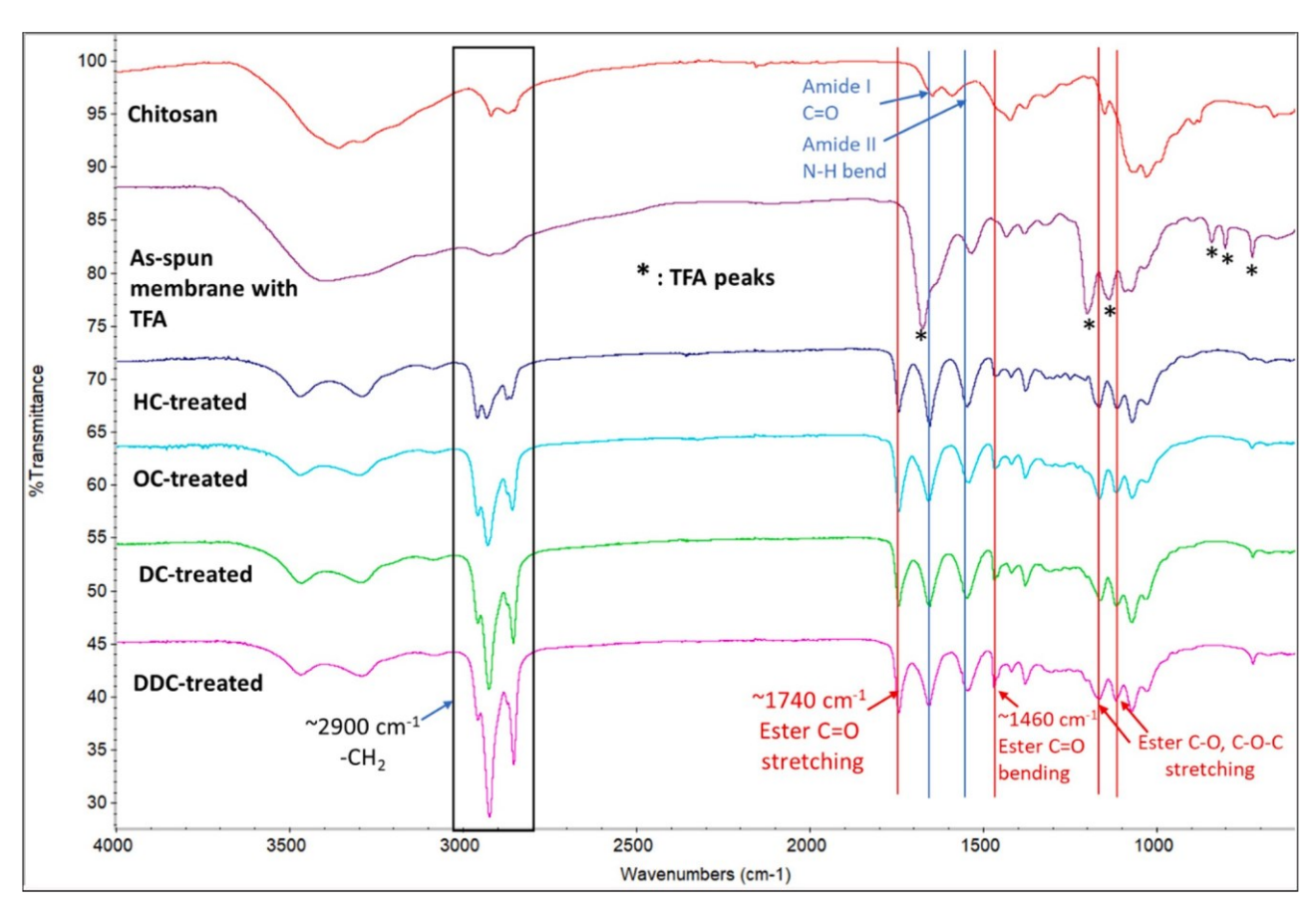


Fig. 1. FTIR spectra of as-spun and acyl-modified chitosan membrane. HC-hexanoyl chloride, OC-octanoyl chloride, DC-decanoyl chloride, DC-decanoyl chloride.

and intensities between chitosan powder and as-spun membrane are primarily due to the presence of TFA salts coupled with their dissimilarities in crystallinity, intramolecular hydrogen bonding and pH because of the presence of -NH $_2$ group in chitosan and -NH $_3$ group in the as-spun membrane. The ammonium trifluoroacetate salt formed during spinning is toxic for the cell, and it reduces the stability of membranes in aqueous environment (Chaoxi Wu et al., 2014). The acylated membranes are missing the peaks corresponding to the TFA salt. However,

the intensity of the peak at $722~\rm cm^{-1}$ increased with the increasing length of the acyl chain (i.e.: methylene group). This peak is due to the rocking vibration of -CH₂ group of the alkyl chain having four or more of methylene group (Smith, 2015). Newly formed peaks at $1745~\rm cm^{-1}$ (for ester C = O stretching), $1460~\rm cm^{-1}$ (for ester C = O bending) and 1120, $1180~\rm cm^{-1}$ (for C–O, C–O-C stretching) confirm O-acylation in the acylated membranes while the increased intensity at $1650~\rm cm^{-1}$ indicates minor N-acylation. Although chitosan amine group is more

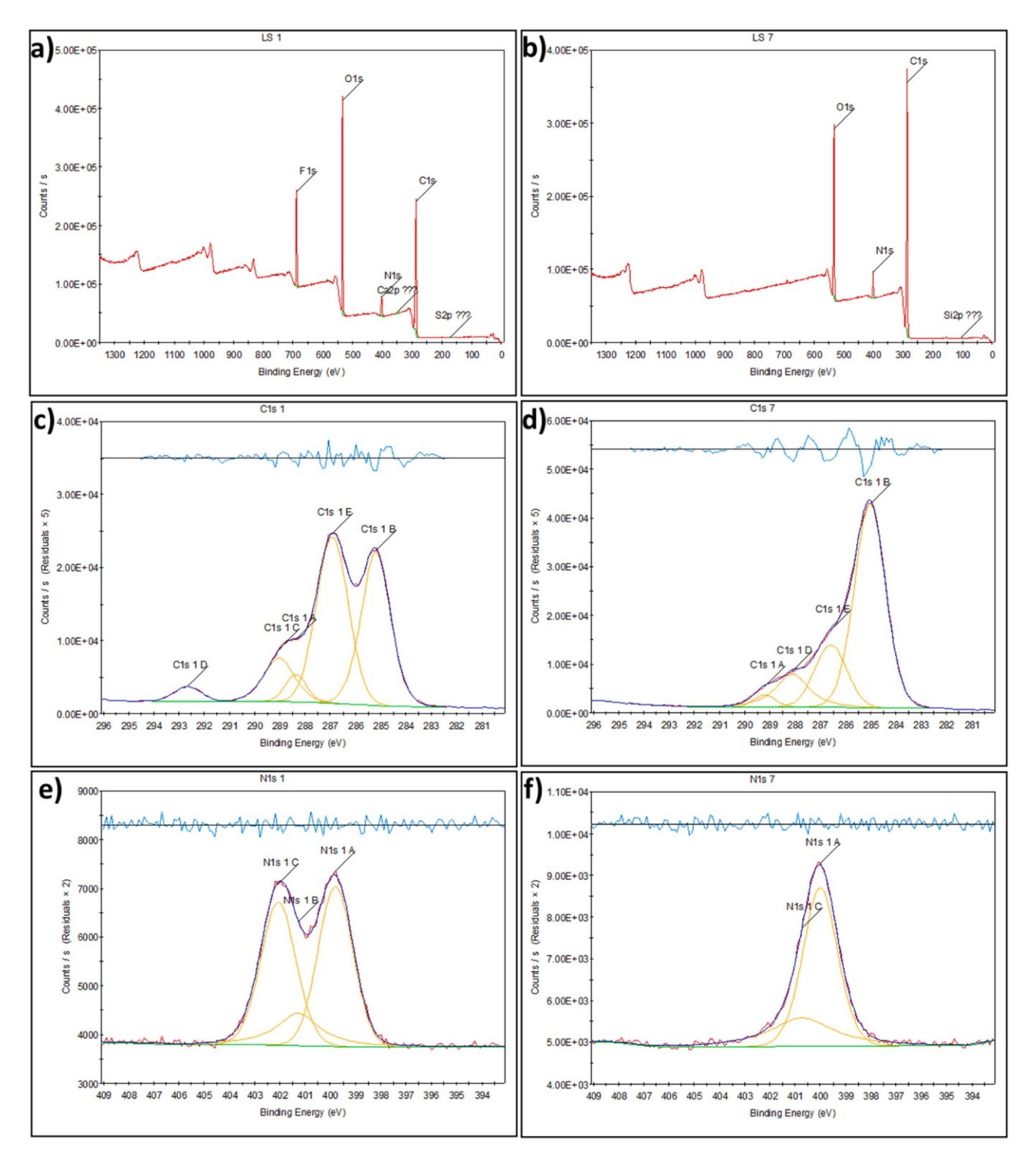


Fig. 2. Full scan spectra of (a) as-spun membrane (b) octanoyl chloride modified membrane, C1s spectra of (c) as-spun membrane (d) ocanoyl chloride modified membrane, and N1s spectra of (e) as-spun membrane, (f) octanoyl chloride modified membrane.

reactive in neutral and acidic conditions, O-acylation dominates over N-acylation in presence of pyridine due to slightly basic environment (Chaoxi Wu et al., 2014). The intensity of the two peaks at 2851 cm⁻¹ and 2951 cm⁻¹ (for asymmetrical and symmetrical bending of methylene group, respectively) increased gradually as the acyl chain length increased from as-spun chitosan membrane to hexanoyl, octanoyl, decanoyl, and dodecanoyl modification (Chaoxi Wu et al., 2014). The hydrophobic fatty acid chain increases the stability of the acylated nanofibrous membrane in aqueous environments allowing the removal of the cytotoxic TFA salt by washing with water (Chaoxi Wu et al., 2014). Moreover, acylated membranes have been found to extend the release of the hydrophobic drug simvastatin from the nanofibrous membrane. The length of the fatty acid chain can also control the release of the drug (Murali et al., 2020). The ester bond has a biological significance in delivering drug molecules into the cells. In an acidic environment or in the presence of bacterial lipase enzymes like in the musculoskeletal injury site, ester bond can break down to release the fatty acid and the loaded drug molecule (Berkmann et al., 2020; Jaeger et al., 1994; Lavis, 2008). Future studies will investigate the release of therapeutics from these modified membranes in the presence or absence

The elemental composition, C1s spectra, and N1s spectra of the asspun and acylated membranes were determined using XPS analysis. Acylated membranes mainly contain carbon, nitrogen, and oxygen (Fig. 2b), while the as-spun membrane has a significant amount of fluorine in the form of ammonium trifluoroacetate salt (Fig. 2a). The membranes might have been exposed to a trace number of impurities in the form of Ca and S during the electrospinning or acylation treatment. Considering the C-C, C-H peak at 284.6 eV (originally 285.2 eV in the sample) as a reference binding energy to correct for 0.6 eV offset due to incomplete charge neutralization of specimens under irradiation from the subsequent C1s peaks and N1s peaks, the as-spun membrane has five peaks in C1s spectra: 286.3 eV (286.9 eV in the Fig. 2c) corresponds to the C-OH and C-OR bond, 287.8 eV (288.4 eV in the Fig. 2c) is due to the presence of C = O bond of the amide group as well as O-C-O bond of the anomeric carbon, 288.4 eV (289.0 eV in the Fig. 2c) and 292.1 eV (292.7 eV in the Fig. 2c) correspond to C = O and C-F bond of the ammonium trifluoroacetate salt (Beamson, 1992). The peaks at 288.4 eV and 292.1 eV disappeared after the acylation and a new peak at 289.1 eV formed which belongs to C = O bond attached to the acyl group (Fig. 2d) (Hammond, Holubka, DeVries & Dickie, 1981). There are three peaks in the as-spun membranes' N1s spectra and two peaks in the acylated membrane. Considering the offset, the acylated membrane has a peak for the amine group (-NH₂) at 399.2 eV and another peak at 400.7 eV for the amide (-NHCOCH₃) group (Fig. 2e). The as-spun membrane has an extra peak at 401.5 eV for ammonium ion (-NH3) present as a trifluoroacetate salt (Fig. 2f). The XPS analysis agrees with the observation of the FTIR analysis that, the TFA salt has been successfully removed from the electrospun membrane and an acyl chain has been added to the membrane through an ester bond.

Elemental analysis was performed on the as-spun and acylated membranes via XPS. Statistical analysis indicates a significant difference in the carbon content among the acylated membranes substituted with different fatty acid chains (P < 0.0001) and the carbon content increased as the length of the substituted chain extends (Fig. 3). The two-way ANOVA analysis indicated a significant difference in the carbon content between 2 h and 5 h reaction groups (p = 0.006). The degree of substitution after 5 h was significantly higher than 2 h and 4 h and it reduced from 3 h to 4 h for C6, C10 and C12 modified ESCM (Fig. 4). However, the differences were statistically insignificant when the time groups were compared separately for each chain length using one-way ANOVA. These changes might be attributed to random changes in the reaction environment. Since acyl chlorides can degrade to corresponding acids in presence of moisture, the surrounding environment can affect the reaction. There was also no significant effect of the chain length on the degree of attachment of the chain (p = 0.08). The degree of

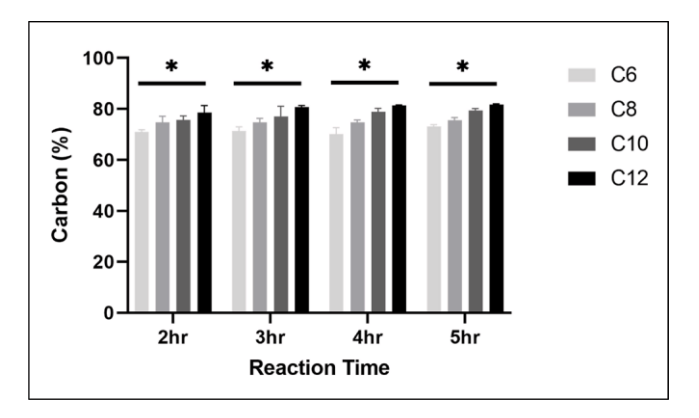


Fig. 3. Bars and error bars represent the mean percentages of atomic carbon in the acylated membranes and standard deviation of the sample respectively (n=3). The asterisks indicate significant differences in carbon content among the acylated membranes based on two-way ANOVA analysis. C6-hexanoyl chloride modified membrane, C8-octanoyl chloride modified membrane, C10-decanoyl chloride modified membrane, C12-dodecanoyl chloride modified membrane.

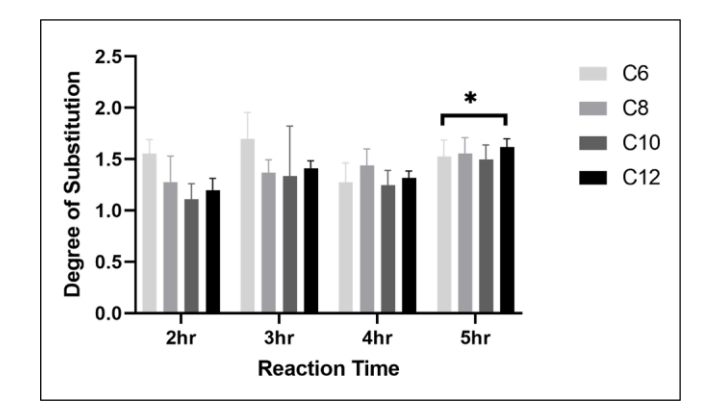


Fig. 4. Bars and error bars represent mean degree of substitution of the fatty acid chain in the acylated membranes and standard deviation of the sample respectively (n=3). The asterisks above the 5hr indicate significant differences in degree of substitution compared to 2hr and 4hr based on two-way ANOVA analysis. C6-hexanoyl chloride modified membrane, C8-octanoyl chloride modified membrane, C10-decanoyl chloride modified membrane, C12-dodecanoyl chloride modified membrane.

substitution was between 1.2–1.6. Theoretically, the maximum degree of O-acylation should be 2 since only the two hydroxyl groups are available for acylation and the amine group of the electrospun membrane is occupied as TFA salt. The reason behind the less-than-theoretical maximum degree of substitution might be the steric hindrance of the attached acyl chains to the coming fatty acids. However, more than 50 % of the fatty acid had been added to the membrane within 2 h, increasing the hydrophobicity of the membrane and stabilizing the nanofibrous structure of the membrane in aqueous environments.

Based on the XPS results and degree of substitution estimation, there was no significant difference in the acylation reaction conducted for different time points. For this reason, ¹H NMR spectra of chitosan and acylated membranes were analyzed for only 5hr reaction group and shown in Fig. 5. The protons denoted by the numbers in red (Fig. 5(f)) are respective to the numbered peaks in Fig. 5 (a, b, c, d). The peak at 2.2 ppm corresponds to protons of -CH₃ on the N-acetyl glucosamine units and the multiple peaks at 3.3–5.5 ppm correspond to the protons of the chitosan ring. The peak pattern of the ring protons for hexanoyl and decanoyl modified membranes have changed from the original chitosan NMR, indicating minor acidic degradation during the dissolution

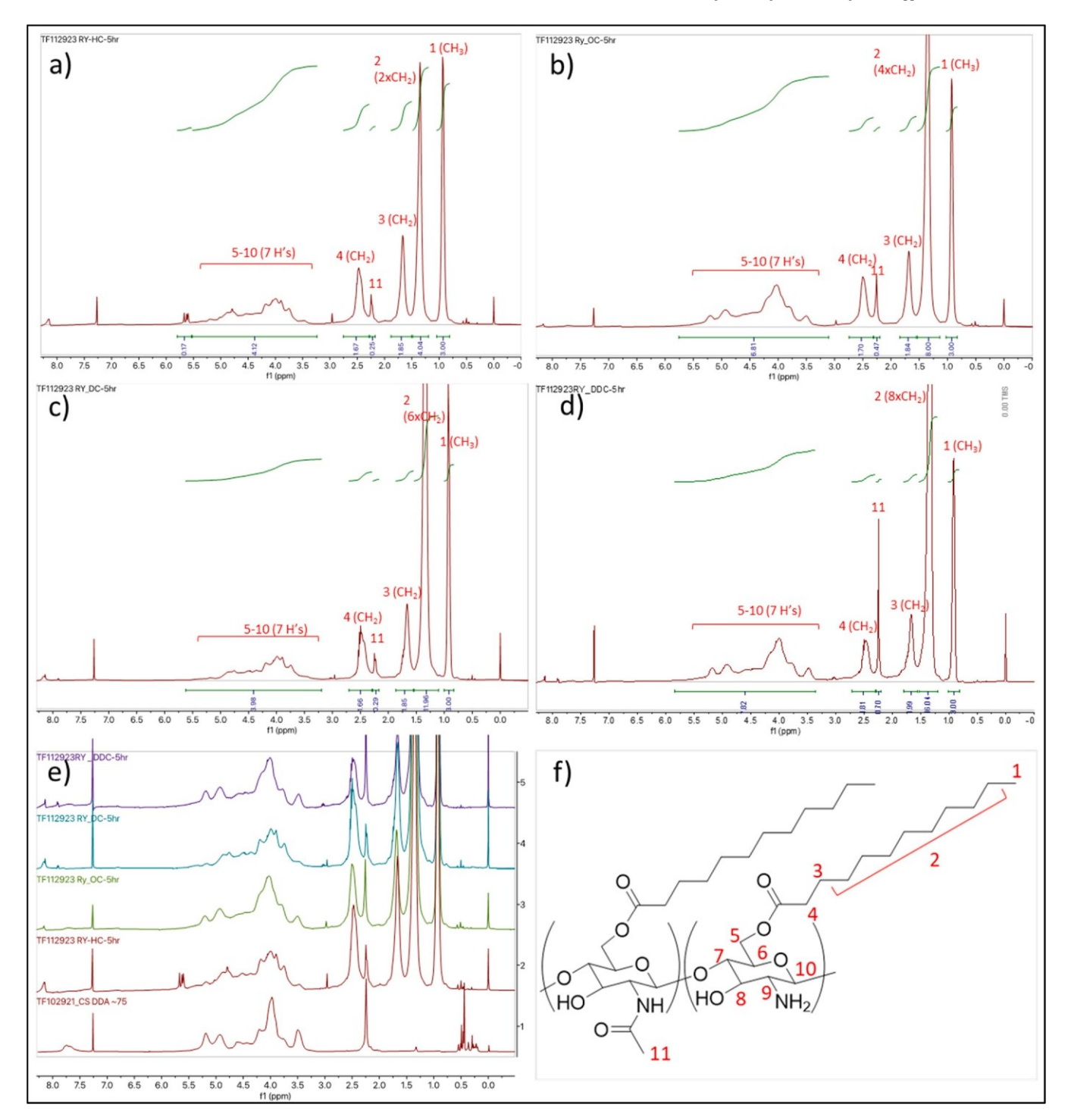


Fig. 5. ¹H NMR spectra of chitosan and acylated membranes dissolved in TFA-d/CDCl₃ solutions. (a) hexanoyl chloride modified membrane (HC), (b) octanoyl chloride modified membrane (OC), (c) decanoyl chloride modified membrane (DC), (d) dodecanoyl chloride modified membrane (DDC), (e) Stacked spectra of chitosan (bottom) and acylated membranes (from top: DDC, DC, DC, HC); reacted for 5hr. (f) chemical structure of dodecanoyl modified membrane with red numbers denoting the corresponding peaks of the acylated membrane spectra.

process. The peaks at 2.5, 1.7, 1.4 and 0.9 ppm are assigned to the protons of the acyl chains and the peak intensity at 1.4 ppm (number 2) varied proportionally to the length of the acyl chain, which further confirms the acylation reaction.

The surface morphology of the as-spun and acylated membranes were examined through SEM (Fig. 6). SEM images show nearly uniform, continuous, and bead-free nanofiber in both as-spun and acylated membranes at different reaction time points. The structural integrity of the membranes is important for their potential applications. The high

surface area and the structural resemblance to the extracellular matrix are two advantageous characteristics of the nanofibrous membrane for its use in drug delivery and tissue engineering. Although the fibrous feature appears to be intact in the images, the diameter has significantly changed after acylation. It was found in the two-way ANOVA analysis that the reaction time did not have a quite significant effect on the fiber diameter (p=0.06), while the attached fatty acid chain length has an extremely significant effect on the fiber size (p<0.0001). The average fiber diameter in the as-spun membrane was 117 \pm 34 nm, which

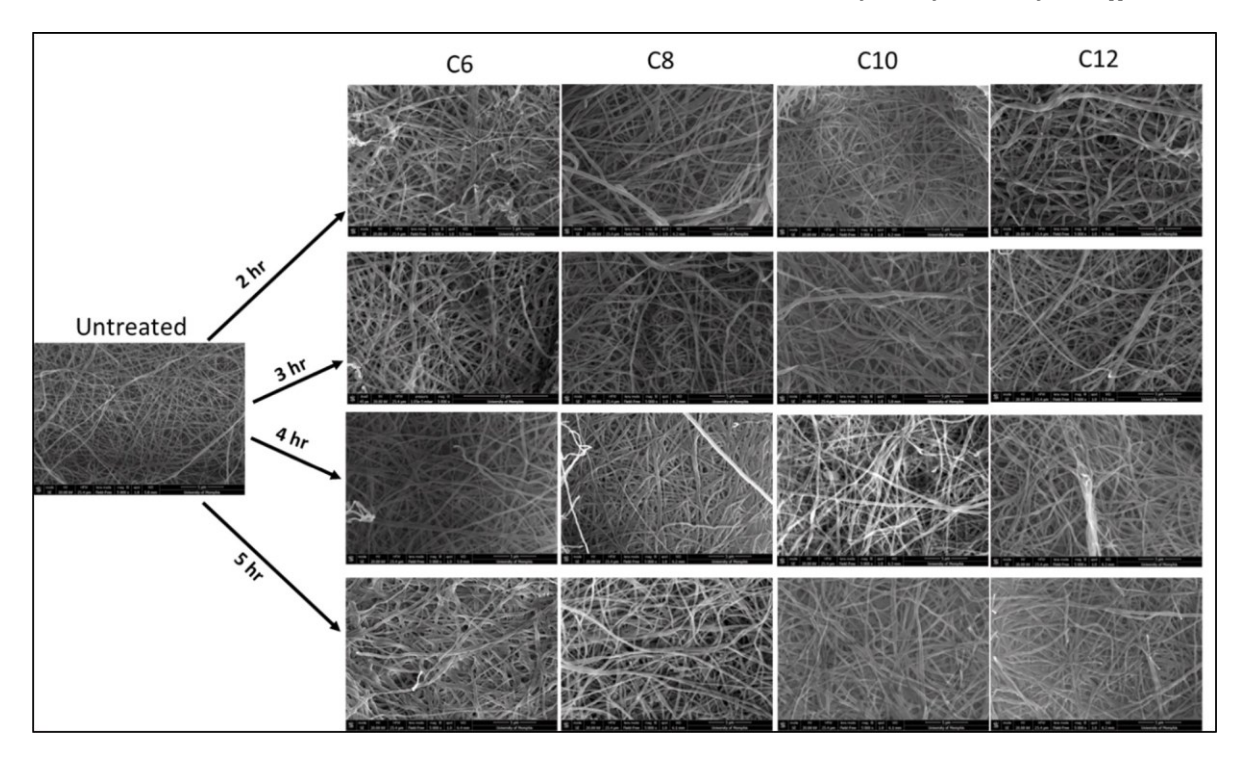


Fig. 6. SEM images of as-spun (untreated) and O-acylated chitosan membranes at different time points at a resolution of 5000x.

enlarged to 189±71 nm in hexanoyl modified, 192±56 nm in octanoyl modified, 209±54 nm in decanoyl modified, and 218±65 nm in dodecanoyl modified membrane (averaging all time points) (Fig. 7). The rising trend of the fiber diameter with the increasing length of the substituted acyl chain has also been observed by Zhang et al. The acyl chains are interdigitated with each other forming a layered structure extending from the main chitosan chain (Le Tien et al., 2003;Zhang et al., 2017). The well-ordered longer chain might form a self-assembled monolayer extending from the surface by hydrophobic interaction, which could result in larger fiber diameter in the longer acyl chain modified membranes.

The wetting properties of the O-acylated membranes were determined by water contact angle measurement (Fig. 8). The contact angle reflects the overall hydrophobicity of the membranes which can imply the attachment of the hydrophobic fatty acid chains confirming the acylation reaction. Water droplets were unstable and absorbed by the as-

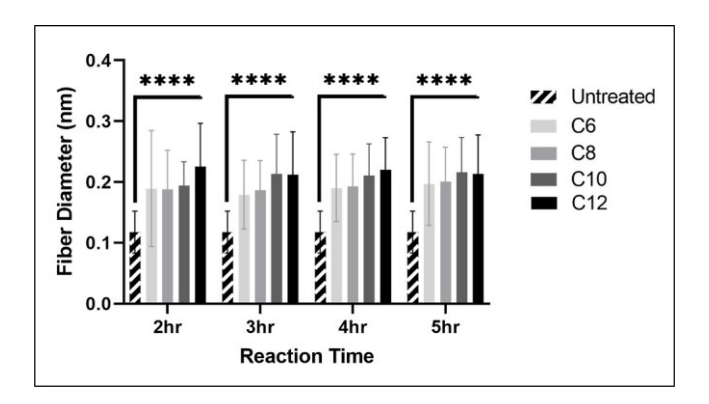


Fig. 7. Bars and error bars represent mean fiber diameters of the membranesas-spun (untreated) and acylated with different fatty acid chain and standard deviation of the sample respectively (n=150). The asterisk signs indicate significant differences in fiber diameter of the acylated fibers compared to the untreated fiber based on two-way ANOVA analysis. C6-hexanoyl chloride modified membrane, C8-octanoyl chloride modified membrane, C10-decanoyl chloride modified membrane.

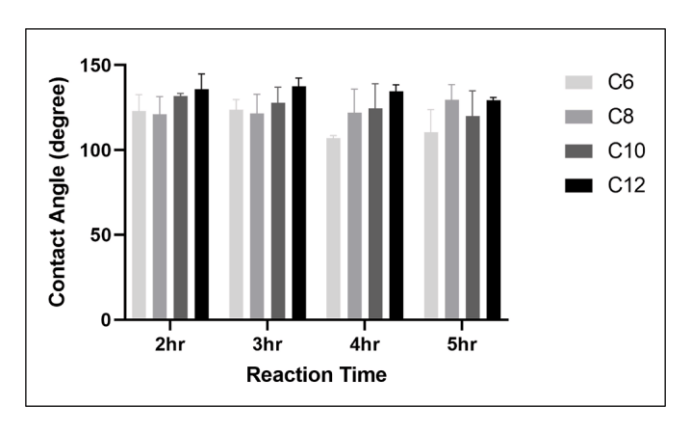


Fig. 8. Bars and error bars represent mean contact angles of the acylated membranes and standard deviation of the sample respectively. C6-hexanoyl chloride modified membrane, C8-octanoyl chloride modified membrane, C10-decanoyl chloride modified membrane, C12-dodecanoyl chloride modified membrane.

spun (untreated) membrane during the contact angle measurement suggesting its overall hydrophilic character. All the other acylated membranes had a contact angle greater than 90° indicating the attachment of the fatty acid chains on the surface of the fibers and resulting in overall hydrophobic properties. The reaction time does not have a considerable impact on the contact angle of the acylated membranes (p = 0.06) indicating that there was similar degree of substitution at all four time points. This implies the maximum degree of attachment of the chain by 2hr. However, there was a significant effect of fatty acid chain length on the contact angle (p < 0.0001). The contact angle of the hexanoyl, octanoyl, decanoyl and dodecanoyl modified membranes were $116.19^{\circ} \pm 4.36^{\circ}$, $123.57^{\circ} \pm 5.67^{\circ}$, $126.12^{\circ} \pm 5.68^{\circ}$ and $134.38^{\circ} \pm 2.73^{\circ}$ respectively (averaging all time groups). The increasing tendency of the contact angle is clearly due to the presence of a higher number of methylene groups in the longer chain since they have similar degrees of attachment of the chains.

as-spun electrospun membranes interact with water extensively due

to their high surface area and presence of hydrophilic groups- residual ammonium TFA salt and hydroxyl group. The large number of polar hydroxyl groups form hydrogen bonds with the water causing swelling and significant deterioration of the nanofibrous structure of the membrane. Meanwhile, the acylation technique reduces the swelling tendency by converting the hydroxyl groups into ester groups and attaching hydrophobic acyl chains which sterically hinders the interaction of the unreacted amine groups with the water, while also removing the toxic TFA salts. This hydrophobic fatty acid can enhance the function of the nanofiber for specific biomedical applications. For example, the hydrophobic chain creates a domain for absorbing and delivering hydrophobic drugs and the drug release profile can be controlled by the length of the chain as well (Murali et al., 2020). Hydrophobically modified nanofibrous membranes can also act as wound coverage significantly accelerating the wound healing process and preventing bacterial infection. (Harrison, Bumgardner, Fujiwara, Baker & Jennings, 2021; C. Wu et al., 2016). A novel fatty acid with therapeutic properties, trans-2-decenoic acid has been incorporated with the chitosan membrane and found to stabilize the membrane as well as reduce the S. aureus and P. aeruginosa biofilm formation while supporting fibroblast growth (Wells et al., 2021).

Conclusions

In this study, the effect of reaction time on the degree of O-acyl substitution on chitosan nanofiber is evaluated using different acyl chlorides of varying lengths. The findings indicated a maximum degree of attachment over 50 % in 2 h of reaction, without significant deterioration of the nanofiber. Earlier approaches of O-acylation have limited use due to low degree of substitution, deleterious reaction condition for fibers, and unavailability of reagents for the attachment of novel fatty acids. The acyl chloride acylation technique is particularly advantageous due to the developed customized route of acyl chloride synthesis from novel therapeutic fatty acids. Therapeutic fatty acids can be attached to the chitosan nanofiber through ester bond that would be cleaved in acidic conditions or in the presence of enzymes, thereby stimulating the release of the therapeutics. Future studies are planned for testing inert reaction conditions, since the acyl chlorides are moisture sensitive. Controlled release of the fatty acids/drug molecules should also be investigated.

CRediT authorship contribution statement

Rabeta Yeasmin: Conceptualization, Formal analysis, Writing – original draft, Writing – review & editing. Ezzuddin Abuhussein: Formal analysis, Writing – original draft, Writing – review & editing. Felio Perez: Formal analysis, Methodology. Tomoko Fujiwara: Conceptualization, Formal analysis. Joel D Bumgardner: Conceptualization, Investigation. Jessica Amber Jennings: Conceptualization, Formal analysis, Funding acquisition, Methodology, Writing – review & editing.

Declaration of competing interest

The authors declare that they have no known competing financial interests or personal relationships that could have appeared to influence the work reported in this paper.

Data availability

Data will be made available on request.

Acknowledgments

We would like to thank Brenna Ballard, Brittany Spencer, and Zoe

Harrison for assistance with experiments and fabricating biomaterials. We would also like to thank Tamanna Ferdous for assisting with FTIR and NMR data acquisition. Thanks are also extended to Omar Skalli for assistance with SEM imaging.

Funding

This research was supported by the National Science Foundation: 1945094

Supplementary materials

Supplementary material associated with this article can be found, in the online version, at doi:10.1016/j.carpta.2024.100443.

References

- Beamson, G. (1992). High resolution XPS of organic polymers. *The scienta esca 300 database*.
- Berkmann, J. C., Herrera Martin, A. X., Ellinghaus, A., Schlundt, C., Schell, H., Lippens, E., & Schmidt-Bleek, K. (2020). Early pH changes in musculoskeletal tissues upon injury-aerobic catabolic pathway activity linked to inter-individual differences in local pH. International Journal of Molecular Sciences, 21(7).
- Berlanga, M., Gomez-Perez, L., & Guerrero, R. (2017). Biofilm formation and antibiotic susceptibility in dispersed cells versus planktonic cells from clinical, industry and environmental origins. Antonie van Leeuwenhoek, 110(12), 1691–1704.
- Borsagli, F. G. M., Carvalho, I. C., & Mansur, H. S. (2018). Amino acid-grafted and N-acylated chitosan thiomers: Construction of 3D bio-scaffolds for potential cartilage repair applications. *International Journal of Biological Macromolecules*, 114, 270–282.
- Fujii, S., Kumagai, H., & Noda, M. (1980). Preparation of poly (acyl) chitosans. Carbohydrate Research, 83(2), 389–393.
- Geng, X., Kwon, O. H., & Jang, J. (2005). Electrospinning of chitosan dissolved in concentrated acetic acid solution. *Biomaterials*. 26(27), 5427–5432.
- Grant, S., Blair, H., & Mckay, G. (1990). Deacetylation effects on the dodecanoyl substitution of chitosan. Polymer Communications.
- Hammond, J., Holubka, J., DeVries, J., & Dickie, R. (1981). The application of x-ray photo-electron spectroscopy to a study of interfacial composition in corrosioninduced paint de-adhesion. *Corrosion Science*, 21(3), 239–253.
- Harrison, Z. L., Bumgardner, J. D., Fujiwara, T., Baker, D. L., & Jennings, J. A. (2021). In vitro evaluation of loaded chitosan membranes for pain relief and infection prevention. *Journal of Biomedical Materials Research. Part B, Applied Biomaterials*, 109 (11), 1735–1743.
- Homayoni, H., Ravandi, S. A. H., & Valizadeh, M. (2009). Electrospinning of chitosan nanofibers: Processing optimization. *Carbohydrate Polymers*, 77(3), 656–661.
- Jaeger, K. E., Ransac, S., Dijkstra, B. W., Colson, C., van Heuvel, M., & Misset, O. (1994).Bacterial lipases. FEMS Microbiology Reviews, 15(1), 29–63.
- Lahiji, A., Sohrabi, A., Hungerford, D. S., & Frondoza, C. G. (2000). Chitosan supports the expression of extracellular matrix proteins in human osteoblasts and chondrocytes. *Journal of Biomedical Materials Research*, 51(4), 586–595.
- Lavis, L. D. (2008). Ester bonds in prodrugs. ACS Chemical Biology, 3(4), 203-206.
- Le Tien, C., Lacroix, M., Ispas-Szabo, P., & Mateescu, M. A (2003). N-acylated chitosan: Hydrophobic matrices for controlled drug release. *Journal of Controlled Release*, 93 (1), 1–13.
- Lin, I. C., Wang, T. J., Wu, C. L., Lu, D. H., Chen, Y. R., & Yang, K. C. (2020). Chitosan-cartilage extracellular matrix hybrid scaffold induces chondrogenic differentiation to adipose-derived stem cells. *Regenerative Therapy*, 14, 238–244.
- Murali, V. P., Fujiwara, T., Gallop, C., Wang, Y., Wilson, J. A., Atwill, M. T., & Bumgardner, J. D. (2020). Modified electrospun chitosan membranes for controlled release of simvastatin. *International Journal of Pharmaceutics*, 584, Article 119438.
- Murali, V. P., Guerra, F. D., Ghadri, N., Christian, J. M., Stein, S. H., Jennings, J. A., & Bumgardner, J. D. (2021). Simvastatin loaded chitosan guided bone regeneration membranes stimulate bone healing. *Journal of Periodontal Research*, 56(5), 877–884.
- Norowski, P. A., Babu, J., Adatrow, P. C., Garcia-Godoy, F., Haggard, W. O., & Bumgardner, J. D. (2012). Antimicrobial activity of minocycline-loaded genipincrosslinked nano-fibrous chitosan mats for guided tissue regeneration. *Journal of Biomaterials and Nanobiotechnology*, 3(04), 528.
- Norowski, P. A., Jr., Fujiwara, T., Clem, W. C., Adatrow, P. C., Eckstein, E. C., Haggard, W. O., & Bumgardner, J. D (2015). Novel naturally crosslinked electrospun nanofibrous chitosan mats for guided bone regeneration membranes: Material characterization and cytocompatibility. *Journal of Tissue Engineering and Regenerative Medicine*, 9(5), 577–583.
- Novikov, V. Y., Derkach, S. R., Konovalova, I. N., Dolgopyatova, N. V., & Kuchina, Y. A. (2023). Mechanism of heterogeneous alkaline deacetylation of chitin: A review. *Polymers*, 15(7).
- Ohkawa, K., Cha, D., Kim, H., Nishida, A., & Yamamoto, H. (2004). Electrospinning of chitosan. Macromolecular Rapid Communications, 25(18), 1600–1605.
- Piechota, M., Kot, B., Frankowska-Maciejewska, A., Gruz ewska, A., & Wo zniak-Kosek, A. (2018). Biofilm formation by methicillin-resistant and methicillin-sensitive Staphylococcus aureus strains from hospitalized patients in Poland. BioMed Research International, 2018, Article 4657396.

- Kumar, Ravi, & V, M. N. (2000). A review of chitin and chitosan applications. Reactive and Functional Polymers, 46(1), 1–27.
- Smith, B. (2015). How to properly compare spectra, and determining alkane chain length from infrared spectra.
- Wells, C. M., Coleman, E. C., Yeasmin, R., Harrison, Z. L., Kurakula, M., Baker, D. L., & Jennings, J. A. (2021). Synthesis and characterization of 2-decenoic acid modified chitosan for infection prevention and tissue engineering. *Marine Drugs*, 19(10).
- Wu, C., Chen, T., Xin, Y., Zhang, Z., Ren, Z., Lei, J., & Tang, S. (2016). Nanofibrous asymmetric membranes self-organized from chemically heterogeneous electrospun
- mats for skin tissue engineering. *Biomedical Materials (Bristol, England), 11*(3), Article 035019.
- Wu, C., Su, H., Tang, S., & Bumgardner, J. D. (2014). The stabilization of electrospun chitosan nanofibers by reversible acylation. *Cellulose (London, England)*, 21(4), 2549–2556
- Zhang, Z., Jin, F., Wu, Z., Jin, J., Li, F., & Wang, Y. (2017a). O-acylation of chitosan nanofibers by short-chain and long-chain fatty acids. *Carbohydrate Polymers*, 177, 203–209.
- Zong, Z., Kimura, Y., Takahashi, M., & Yamane, H. (2000). Characterization of chemical and solid state structures of acylated chitosans. *Polymer*, 41(3), 899–906.